Walisongo Journal of Chemistry
Walisongo Journal of Chemistry Vol. 9 Issue 1 (2026), 67-75
ISSN: 2621-5985 (online); 2549-385X (print)
DOI: https://doi.org/10.21580/wjc.v9i1.31598

MICROSTRUCTURAL CHARACTERIZATION OF BIOCHAR–CHITOSAN COMPOSITES LOADED WITH NITROGEN AND Fe FOR SLOW-RELEASE FERTILIZER APPLICATIONS

Martasiana Karbeka*, Agnes Lema, Jublina Padalegi

Department of Chemistry, Faculty of Mathematics and Natural Sciences, Universitas Tribuana Kalabahi

*Corresponding author: karbekamartasiana@gmail.com

Abstract

Nutrient-use efficiency in agricultural fertilization remains very low because nitrogen is readily lost through leaching and volatilization. Biochar and chitosan can be used as nutrient-coating materials to modify nutrient-release rates and improve fertilization efficiency. This study evaluates the structural and elemental characteristics of chitosan–biochar slow-release fertilizers by comparing BCB@N and BCB@N/Fe composites. Particle size analysis showed an increase in average particle size from 430.18 ± 19.60 µm for BCB@N to 485.48 ± 62.64 µm for BCB@N/Fe. EDX data revealed high percentages of carbon and silica in BCB@N, confirming a porous framework, whereas BCB@N/Fe exhibited elevated oxygen and calcium levels, indicating the formation of Fe–chitosan complexes and the coprecipitation of Ca ions. TEM imaging confirmed that this chemical modification transformed the open internal microstructure of BCB@N into a significantly denser surface in BCB@N/Fe. Accordingly, the smaller particle size and open structure of BCB@N may facilitate faster water diffusion and earlier nutrient release, while the denser structure and larger particle size of BCB@N/Fe may provide a stronger barrier to water diffusion and support slower, more controlled nutrient release.

Keywords: *biochar; chitosan; nitrogen; slow-release fertilizer; biodegradability*

Introduction

In developing an effective modern fertilization system that minimizes nutrient loss to the environment, research on slow-release fertilizers is essential. Urea prill fertilizer, with a nitrogen content of 46%, is not sufficiently efficient to support plant growth because conventional urea prills are easily washed away, causing the released nitrogen to dissolve and be transported by water (1,2). In addition, nitrogen is volatile and can undergo denitrification in the environment. These conditions indirectly increase the required urea dosage, which in turn contributes to environmental pollution, particularly soil and water degradation. Therefore, the use of slow-release fertilizers is highly promising because it can increase nitrogen uptake by plants, reduce nitrogen loss to the environment, improve fertilizer-use effectiveness and efficiency, and indirectly reduce pollution levels (3,4).

Many studies have been conducted on slow-release fertilizers; however, several limitations remain, particularly regarding the type of material selected as the coating. The coating material plays an important role in the effectiveness of controlled nutrient release; therefore, material selection is crucial in the development of slow-release fertilizers. Conventional SRF development often uses synthetic polymers that are difficult to decompose, leaving residues that cause problems in agricultural soils. Natural polymers have gained increasing interest as environmentally friendly coating materials for agricultural applications. Among these materials, chitosan is considered one of the most promising biopolymers because of its biodegradability, biocompatibility, non-toxicity, and excellent film-forming properties. These characteristics make chitosan a potential coating material for the development of slow-release fertilizers (SRFs), enabling improved nutrient-use efficiency while minimizing environmental impacts (5,6). Chitosan biopolymers are biodegradable and porous materials that can be used as storage media. They also contain active groups that can increase binding capacity. However, chitosan has low mechanical strength and exhibits hydrophilic properties, although it is insoluble in water at neutral pH and dissolves only under acidic conditions (7). Meanwhile, the use of chitosan as a coating material in SRFs remains largely limited to single-nutrient fertilizers containing only one essential nutrient, namely nitrogen, and has not been widely applied in the development of compound fertilizers containing essential macro- and micronutrients (4,8). In addition to chitosan, biochar has potential as an SRF coating material because its high organic carbon content can support soil improvement. Various studies have also demonstrated the role of biochar in improving soil properties (9–11). However, studies on chitosan–biochar composites for fertilizer-coating materials have not been conducted systematically, particularly for nitrogen–Fe fertilizers. The biochar–chitosan combination is a porous material with high porosity that supports nutrient adsorption capacity; however, because of this high porosity, the composite also has a high diffusion rate (12–14). This limitation can be overcome by adding metals, such as Fe, to biochar–chitosan composites to form coordination bonds with amine or carboxylate groups, resulting in a more compact and dense structure (15,16).

Previous studies have mainly focused on two-component systems, such as chitosan–N or chitosan–Fe, while the four-component chitosan–biochar–N system with added Fe has not been widely studied. Therefore, understanding the hybrid structure in relation to slow-release fertilizers is important. Various approaches were used to characterize the structural components of the fertilizer-coating system, including particle size analysis (PSA), energy-dispersive X-ray spectroscopy (EDX), and transmission electron microscopy (TEM). Although research on the development of slow-release fertilizers continues to expand, achieving optimal fertilization efficiency while mitigating environmental leaching remains constrained by the structural limitations of single-layer coatings. The use of a chitosan–biochar hybrid composite as a dual-coating system offers a promising strategy to overcome these drawbacks; however, a comprehensive understanding of its structural characteristics and mechanistic performance remains limited. Therefore, this study aims to evaluate the structural properties of this hybrid composite to elucidate its efficacy as a dual-coating matrix. This work demonstrates the significant potential of chitosan–biochar systems in controlling nutrient release and improving fertilization efficiency.

Experimental Section

Materials

The materials used in this study were 2% acetic acid (Sigma-Aldrich, Merck), chitosan (Sigma-Aldrich, Merck), biochar, urea, and distilled water.

Instruments

The instruments used in this study were a particle size analyzer (PSA; Shimadzu SALD-7500, 0.01–2500 μm), energy-dispersive X-ray spectroscopy (EDX; JEOL JSM-6510LA, 0.5–30 kV), and transmission electron microscopy (TEM; JEM-2100Plus JEOL, 20–200 kV).

Research Procedure

Sample Preparation

The chitosan solution was prepared by dissolving chitosan in 2% acetic acid to produce chitosan gel. Iron sand, as the Fe source, was first crushed using a mortar and sieved to a size of 250 mesh. Biochar was obtained from the pyrolysis of rice husks and sieved to a size of 250 mesh.

Synthesis of SRF Beads

The chitosan gel was prepared in the first container and stored. In the second container, 3 g of urea as the nitrogen source was dissolved in 15 mL of water, and 3 g of biochar was dispersed into the solution while stirring with a magnetic stirrer for 30 min. The mixture in the second container was added to the first container containing the stirred chitosan gel until a homogeneous mixture was obtained. The resulting mixture was placed in a syringe and slowly dripped into 1 M NaOH to induce solidification and form biochar–chitosan–urea (BCB@N) beads. The beads were neutralized and dried at room temperature. The same process was used to synthesize beads with added Fe to form biochar–chitosan–urea–Fe (BCB@N/Fe) beads.

Characterization

The resulting BCB@N and BCB@N/Fe beads were characterized using several instruments.

PSA Characterization

The sample was dispersed in distilled water to ensure homogeneity and prevent agglomeration. Particle size distribution measurements were conducted at room temperature (25°C) with a scattering angle of 90°. The results are presented as mean particle size distribution curves to evaluate the structural uniformity of the coating material.

EDS Characterization

The sample was dried in a vacuum oven and coated with a thin carbon layer to enhance electrical conductivity. Analysis was performed at an accelerating voltage of 15–20 kV with a working distance (WD) of approximately 10 mm. The elemental mapping results were used to confirm the presence and distribution of constituent elements within the sample matrix.

TEM Characterization

The sample was ground into a fine powder and subsequently dispersed in ethanol via sonication for 15 min. The resulting suspension was then deposited onto a carbon-coated copper grid. Microscopic observations were carried out at accelerating voltages ranging from 120 to 200 kV to obtain high-resolution images of the coating morphology and internal porosity of the matrix.

Results and Discussion

SRF beads were successfully synthesized through a solidification process and then characterized.

Figure 1. Solidified beads

Particle Size Distribution

The particle size distributions of the BCB@N and BCB@N/Fe composites were analyzed, with each sample measured in triplicate. The average size values are shown in Tables 1 and 2, while the particle size distribution curves are shown in Figures 2 and 3.

Table 1. Average size of BCB@N SRF beads

Measurement 1	446.03 µm
Measurement 2	432.25 µm
Measurement 3	412.27 µm
Average BCB@N	430.18 ± 19.60 µm

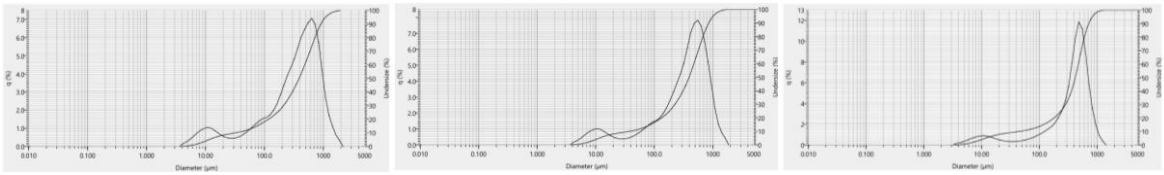

Figure 2. Particle size distribution of BCB@N

Table 2. Average size of BCB@N/Fe SRF beads

Measurement 1	498.34 µm
Measurement 2	425.96 µm
Measurement 3	532.14 µm
Average BCB@N/Fe	485.48 ± 62.64 µm

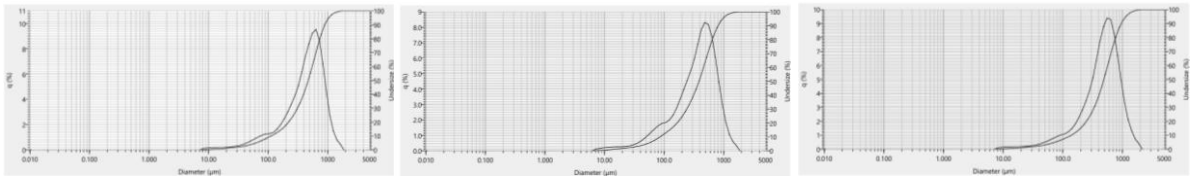

Figure 3. Particle size distribution of BCB@N/Fe

The PSA results showed that the average particle size of BCB@N was 430.18 ± 19.60 µm, while that of BCB@N/Fe was 485.48 ± 62.64 µm. Compared with BCB@N, the BCB@N/Fe composite had a significantly larger particle size, which was driven by the successful introduction of iron species. The added Fe interacted with chitosan and biochar through complex formation via cross-linking with the chitosan polymer. This cross-linking formed larger macromolecules and increased the density of BCB@N/Fe. Based on the average particle size data, the standard deviation of BCB@N/Fe was greater than that of BCB@N, with values of ±62.64 µm and ±19.60 µm, respectively. This indicates that the bead synthesis process produced less uniform beads because of the formation of Fe oxide aggregates in the chitosan–biochar matrix composite as the coating material.

The substitution of Fe from iron sand incorporated into the chitosan polymer strongly affected the size and morphology. Transition metal ions act as cross-linking agents through coordination bonds with amino and carboxylate groups present in chitosan and biochar, resulting in larger particle sizes and higher mechanical stability in the chitosan polymer system. Cross-linking between metal ions and carboxylate groups is consistent with reported mechanisms for silica–magnetite adsorbents, in which surface OH groups are cross-linked with Fe–O groups on the magnetite surface (16,17).

The BCB@N composite had a smaller particle size distribution because no Fe from iron sand was added; therefore, Fe oxide aggregates were not formed, resulting in smaller particle sizes. In relation to its potential as a slow-release fertilizer

material, the smaller size of BCB@N can increase the surface area of the material, allowing the nutrient-release mechanism to occur more rapidly. In contrast, the larger BCB@N/Fe composite may release nutrients more slowly because the larger particle size lengthens the nutrient diffusion pathway. Thus, the addition of Fe to the slow-release fertilizer system not only enriches the nutrient content but also contributes to controlling nutrient release through changes in particle size.

EDX Characterization

To identify the elemental composition of the BCB@N and BCB@N/Fe composites, EDX analysis was conducted. Based on the EDX data, the binding of urea and Fe in the chitosan–biochar matrix can be analyzed. The EDX results are shown in Table 3 and Figure 4.

Table 3. Elemental composition of BCB@N and BCB@N/Fe

Element	Percentages	
	BCB@N	BCB@N/Fe
C	64.74	47.19
O	32.10	45.59
Na	1.06	1.05
Mg	0.75	0.96
Si	3.55	0.36
Ca	0.46	4.85
Cu	0.88	-

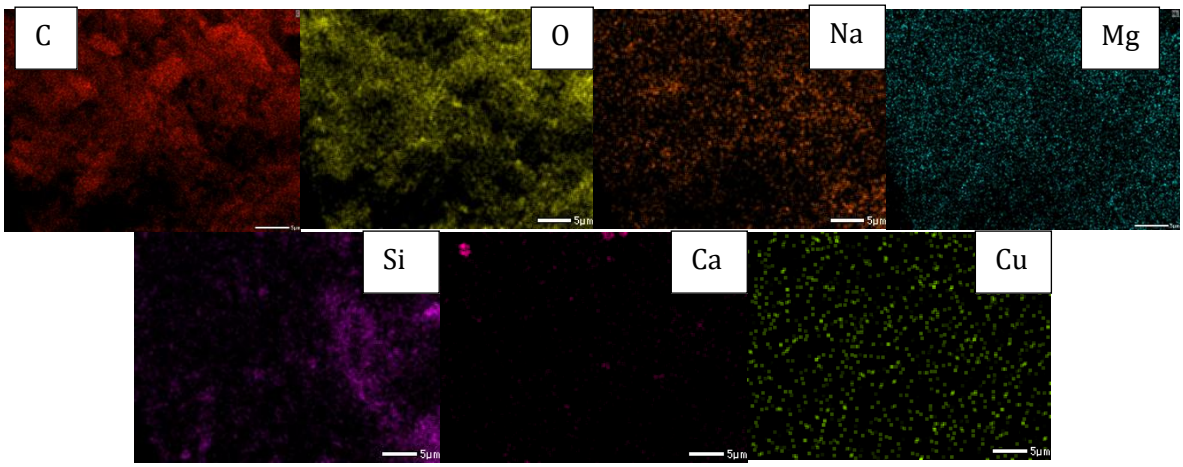

Figure 4. Elemental composition of BCB@N and BCB@N/Fe

Based on the characterization results of the constituent element percentages, significant differences were observed in the elemental composition of BCB@N and BCB@N/Fe. BCB@N was dominated by carbon and oxygen, with percentages of 64.74% and 32.10%, respectively. This result is consistent with the composition of the BCB@N composite, which consists of chitosan, biochar, and

nitrogen, where carbon and oxygen are the main elements of the chitosan–biochar structure. The small amount of Si content (3.55%) indicates the presence of silicate minerals from biochar. Several minor elements with percentages below 1%, such as Na, Mg, Ca, and Cu, were impurity minerals produced during the chitosan–biochar synthesis process. In BCB@N/Fe, the carbon content decreased to 47.19%, while the oxygen content increased to 45.59%.

Fe was not detected by EDX because the electron beam penetrates and excites X-rays only from a depth of 1–2 μm (18), whereas Fe was located within the core matrix of the chitosan–biochar-based SRF. This dual-layer coating system was further confirmed by TEM analysis (see Figure 5).
The increased oxygen content in BCB@N/Fe is attributed to the presence of iron oxide phases, such as Fe3O4 and Fe2O3. In addition, this increase was enhanced by cross-linking between Fe–O groups and the abundant amine, hydroxyl, and carboxyl functional groups provided by chitosan and biochar (13,16).

The increased oxygen level also supports the formation of chitosan–Fe complexes through cross-linking. A significant increase in Ca ions was observed in BCB@N/Fe compared with BCB@N, from 0.46% to 4.85%. These data strengthen the indication of Fe involvement because Fe in the BCB@N/Fe composite can trigger coprecipitation with Ca ions, thereby increasing the strength of the composite structure. Silicate minerals decreased because of silicate dispersion by Fe as a result of Fe–chitosan bond formation, which made the matrix denser and more compact. Other minerals, such as Na and Mg, were present as impurities. Cu was not detected in BCB@N/Fe, likely because its signal was masked by the modified Fe-containing matrix. In BCB@N composites dominated by carbon and silicate, the resulting structure was more open and porous, accelerating the nutrient-release process. In BCB@N/Fe composites, the increases in oxygen and calcium contributed to the formation of a denser matrix with stronger mechanical bonding properties, resulting in reduced porosity and slower nitrogen diffusion.

These results show that BCB@N/Fe composites can increase the density and mechanical strength of chitosan polymers and have potential for the development of slow-release fertilizers. This finding is consistent with research showing that biochar-based slow-release nitrogen fertilizers with added Ni (SRF-Ni) produce a non-uniform structure but increase matrix density, thereby reducing the pore surface area (19).

TEM Characterization

Observation of the internal microstructure can provide a clear picture of aggregation patterns, porosity, and nitrogen–Fe interactions in the chitosan–biochar matrix. High-resolution TEM images can provide information on the relationship between the internal structure of the composite and its functional properties, which are important for the development of slow-release fertilizers (20). TEM images showing the internal morphology of the BCB@N and BCB@N/Fe composites are presented in Figure 5.

Based on the TEM images in Figure 5, significant structural differences were observed between the BCB@N and BCB@N/Fe composites. The TEM images of the BCB@N composite showed low-to-moderate-contrast aggregates because of the non-homogeneous distribution of chitosan and biochar, which was clearly visible at magnifications of 100× and 200×. This finding is consistent with the composition of the BCB@N composite, which consists of nitrogen-containing chitosan–biochar. At 500× magnification, the formed aggregates appeared porous, with a diffuse amorphous structure commonly found in chitosan composite systems, making the internal morphology of BCB@N more open. The internal microstructural characteristics of BCB@N strongly indicate that the interaction

formed was mainly physical, with a less dense structure, resulting in faster nitrogen diffusion.

Figure 5 shows that BCB@N/Fe had aggregates with more intense dark contrast, which was clearly visible at magnifications of 100× and 200×. The darker contrast is characteristic of iron or iron oxide particles with high electron density. At 500× magnification, the morphology of BCB@N/Fe clearly formed solid agglomerates originating from iron-sand Fe particles measuring hundreds of nanometers and distributed as clusters. The presence of Fe particles increased compaction, aggregate density, and structural regularity. The functional properties of the BCB@N/Fe microstructure are associated with nucleation through coordination and electrostatic interactions between Fe and the amino groups of chitosan and the carboxylate groups of biochar, which trigger compaction of the BCB@N/Fe composite. This compaction causes the BCB@N/Fe composite matrix to become denser, resulting in decreased porosity and narrower intraparticle diffusion pathways, which may slow the rate of nitrogen release.

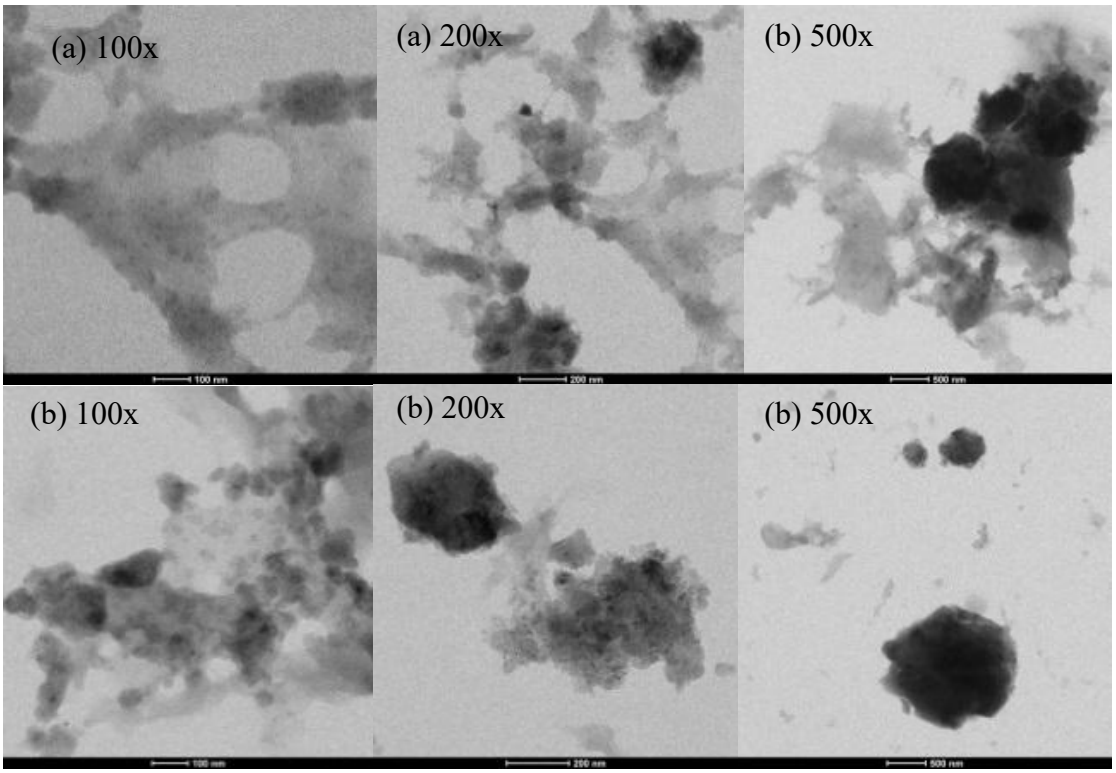

Figure 5. TEM images of (a) BCB@N and (b) BCB@N/Fe

Conclusion

BCB@N and BCB@N/Fe composites based on chitosan–biochar had average particle sizes ranging from 430.18 ± 19.60 µm to 485.48 ± 62.64 µm, with Fe addition increasing the overall granule dimensions. The high percentages of carbon and silica in BCB@N confirm a well-developed porous framework suitable for nutrient retention. Chemical modification through Fe impregnation transformed this open internal microstructure into a significantly denser surface in BCB@N/Fe, as confirmed by TEM imaging. This transition was driven by the successful formation of Fe–chitosan complexes and the coprecipitation of Ca ions, which were supported by the elevated oxygen and calcium levels observed in the EDX analysis. The diversity of these functional interactions and the denser matrix morphology strengthen structural

stability, creating potential reactive sites for controlled nutrient management. Overall, these distinct structural and elemental characteristics make BCB@N and BCB@N/Fe highly promising for improving nutrient-release efficiency gradually, thereby supporting increased fertilizer efficiency and agricultural sustainability.

Acknowledgement

This work was supported by the Ministry of Education, Science, and Technology, Directorate General of Research and Development, under Number 0488/C/DT.06.01/2025 concerning recipients of publication assistance in reputable journals in 2025.

References

[1] Manzoor S, Habib-ur-Rahman M, Haider G, Ghafoor I, Ahmad S, Afzal M, et al. 2022. Biochar and slow-releasing nitrogen fertilizers improved growth, nitrogen use, yield, and fiber quality of cotton under arid climatic conditions. *Environ Sci Pollut Res*. 29(9), 13742–55.

[2] Sandeep Jakkula V, Wani SP. 2018. Zeolites: Potential soil amendments for improving nutrient and water use efficiency and agriculture productivity. Sci Revs Chem Commun. 8(1),119.

[3] Hartatik W, Mardliyati E, Wibowo H, Sukarto A, Yusron Y. 2020. Formulasi dan Pola Kelarutan N Pupuk Urea-Zeolit Lepas Lambat. J Tanah dan Iklim. 44(1),61-70.

[4] Lestari S, Yuningsih LM, Muharam S, Kimia PS, Sains F, Sukabumi UM. 2022. Hidrogel Superabsorben Berbasis Natrium Alginat-Bentonit sebagai Pelapis Pupuk Lepas Lambat. J Ris Kim. 13(1),58–67.

[5] Fatma Nur Parin , Kenan Yildirim PT. 2020. Biochar loaded chitosan/gelatin/poly(ethylene glycol) biocomposite beads: Morphological, thermal and swelling properties. J Innov Sci Eng. 4(2),56–68.

[6] Rahmayani RFI, Arryanto Y, Kartini I. Pengaruh Metode Pencampuran pada Pembuatan Komposit Kitosan-Zeolite-Fe terhadap Pelepasan Fe(III). 2019. *JKPK (Jurnal Kim dan Pendidik Kim*. 4(3),205–15.

[7] Herianus M, Loth B, Zakarias A M. 2024. Membranes with Chitosan-Chitosan/*Phthalate* Matrix and Montmorillonite-Carbon Nanotubes Filler for DMFC Applications. *Indones Chim Acta*. 17(1),37–46.

[8] Finalis ER, Sri Djangkung SM, Arfiana, Ilhamsyah Noor, Suratno H, Rosyadi E, et al. 2020. Development of Carbon Based NPK Slow Release Fertilizer using Biochar from Oil Palm Empty Fruits Bunch. *Indones J Energy*. 3(1),19–24.

[9]. Griselda M, Hamzah A, Fikrinda W, Priyadarshini R, Lestari SU, Tunggadewi UT, et al. P*rosiding Seminar Nasional Lahan Suboptimal ke-12 Tahun 2024, Palembang 21 Oktober 2024 "Revitalisasi Lahan Suboptimal Secara Berkelanjutan Berbasis Pertanian Presisi dan Pemberdayaan Petani Milenial* ". In: Penggunaan Biosan (Biochar dan Kitosan) terhadap Pertumbuhan Tanaman Kangkung (Ipomoea reptans) dan Pengendalian Cu. Palembang; 2024. p. 374–82.

[10] Martasiana Karbeka LL dan DL. Pengaruh Penggunaan Biochar Sekam Padi Dan Bokashi Sebagai Pembenah Sifat Kimia Tanah. *Seminar Nasional Kimia Dan Pendidikan Kimia I, Kupang 31 Maret 2022*. Kupang: Universitas Nusa Cendana; 2022. p. 28–34.

[11] Zakarias Mautuka, Astriana Maifa MK. 2022. Pemanfaatan Biochar Tongkol Jagung Guna Perbaikan Sifat Kimia Tanah Lahan Kering. *J Ilm Wahana Pendidik*.. 8(3),178–83.

[12] Yu Y, Liu W, Zhang Y, Zhang B, Jin Y, Chen S, et al. 2024. Chitosan/magnetic biochar composite with enhanced reusability: Synergistic effect of functional groups and multilayer

structure. *Arab J Chem*. 17(5),105746.

[13] Martasiana Karbeka, Zakarias Mautua DOTL. 2024. Sintesis Pupuk Lepas Lambat Berbasis Kitosan Biochar Urea Sebagai Material Potensial Pelepasan Nitrogen. *lantanida J*. 12(2),113–23.

[14] Wang C, Luo D, Zhang X, Huang R, Cao Y, Liu G, et al. 2022. Biochar-based slow-release of fertilizers for sustainable agriculture: A mini review. Environ Sci Ecotechnology. 10:100167.

[15] Karbeka M, Nuryono, Suyanta. 2020. Synthesis of silica coated on iron sand magnetic materials modified with 2-mercaptobenzimidazole through sol-gel. Moroccan J Chem. 8(S1),44–52.

[16] Rafique MI, Al-wabel MI, Al-farraj ASF, Ahmad M, Aouak T, Al-swadi HA, et al. 2025. Incorporation of biochar and semi- interpenetrating biopolymer to synthesize new slow release fertilizers and their impact on soil moisture and nutrients availability. Sci Rep. 15,1–15.

[17] Karbeka M, Nuryono, Suyanta. Coating of mercapto modified silica on iron sand magnetic material for Au(III) adsorption in aqueous solution. IOP Conf Ser Mater Sci Eng. 2020;823(1):1–8.

[18] Joseph I. Goldstein , Dale E. Newbury , Joseph R. Michael , Nicholas W.M. Ritchie , John Henry J. Scott DCJ. Scanning Electron Microscopy and X-Ray Microanalysis. Springer; 2018.

[19] Herlina N, Nuryani S, Utami H, Nurudin M, Hanudin E. 2025. Synthesis and characterization of slow release fertilizer nitrogen and slow release fertilizer potassium based on biochar with nanotechnology and alginate. *J Ecol Eng.* 226(6),378–90.

[20] Xu X, Yu Z, Chen W, Chen A, Motta A, Wang X. Automated analysis of grain morphology in TEM images using convolutional neural network with CHAC algorithm. *J Nucl Mate*r . 2024;588(July 2023):154813.